Confinement from merons

F. Lenz,[1] J. W. Negele,[2] and M. Thies[1]

[1]*Institute for Theoretical Physics III, University of Erlangen-Nürnberg, Staudstrasse 7, 91058 Erlangen, Germany*
[2]*Center for Theoretical Physics, Laboratory for Nuclear Science, and Department of Physics, Massachusetts Institute of Technology, Cambridge, Massachusetts 02139, USA*

It is shown that an effective theory with meron degrees of freedom produces confinement in SU(2) Yang-Mills theory. When the scale is set by the string tension, the action density and topological susceptibility are similar to those arising in lattice QCD. The potential for this effective theory to produce center symmetry in SU(2) is discussed.

I. INTRODUCTION

Although confinement is one of the most striking and fundamental phenomena that arises from the deceptively simple QCD Lagrangian, its physical mechanism has yet to be understood. One important element is sufficient disorder to drive a large Wilson loop to produce an area law as seen, for example, in the strong coupling expansion of lattice QCD, which produces an area law already in lowest order. However, disorder alone is not the whole story, as evidenced by the fact that the strong coupling expansion also erroneously yields confinement in U(1) gauge theory. A second important feature is center symmetry. By gauge fixing in continuum QCD up to a residual center symmetry or in lattice QCD by multiplying all the links in the time direction on a single time slice by an element of the center, it follows that the effective action has the symmetry $S_{eff}(P) = S_{eff}(\mathcal{Z}P)$, where P denotes a Polyakov loop and $\mathcal{Z}$ is a center element [1,2]. A serious candidate for the confinement mechanism should have the potential of realizing this symmetry. One appealing analytical approach to understanding nonperturbative QCD is expansion of the path integral for the partition function around stationary classical solutions and evaluating the fluctuations around these solutions. The development of highly successful instanton liquid models and the observation of instantons and their zero modes in lattice QCD have provided clear insight into how chiral symmetry breaking arises in QCD [3,4]. However, singular gauge instantons fail to produce confinement and, as will be seen below, also fail to produce center symmetry.

In this work we reexamine the possibility that merons, another set of solutions to the classical field equations, can produce confinement. As noted long ago [5], merons are sufficiently disordering that they have the potential to produce confinement. In contrast to instantons, whose gauge fields fall off as r^{-3} in singular gauge, merons can only be written in regular gauge with fields that decrease as r^{-1}. In the absence of correlations between distant merons, this long-range gauge field would give rise to an unphysical background field. Since analytic treatment of these correlations appears to be intractable, the behavior of meron ensembles has not previously been analyzed.

In SU(N) gauge theories, the deconfinement transition is associated with a symmetry property. Center symmetry, a residual discrete gauge symmetry, is realized in the confined phase and broken in the deconfined phase. In SU(2), center symmetry transformations change the sign of the Polyakov loop, defined in the compact t direction as

$$P(x,y,z) = \frac{1}{2} \text{tr } P \exp\left\{ i \oint dt A_0(x,y,z,t) \right\}.$$

The realization of the center symmetry implies the vanishing of the expectation value of the Polyakov loop which in turn guarantees an exponential decrease in the Polyakov loop correlator related to confinement. In the deconfined phase, the Polyakov loop expectation value is finite. The Polyakov loop thus serves as an order parameter. In the construction of ensembles of field configurations with which to explore confinement, it is useful to study the Polyakov loop of the building blocks. As Fig. 1 shows, unlike the winding number, the asymptotic value of the Polyakov loop of an instanton is not changed in the tunneling process and is identical for instantons and anti-instantons. Thus, tunneling processes do not give rise to a coherent superposition of fields with opposite values of P so that a center-symmetric ensemble of field configurations cannot be generated in a natural way by the
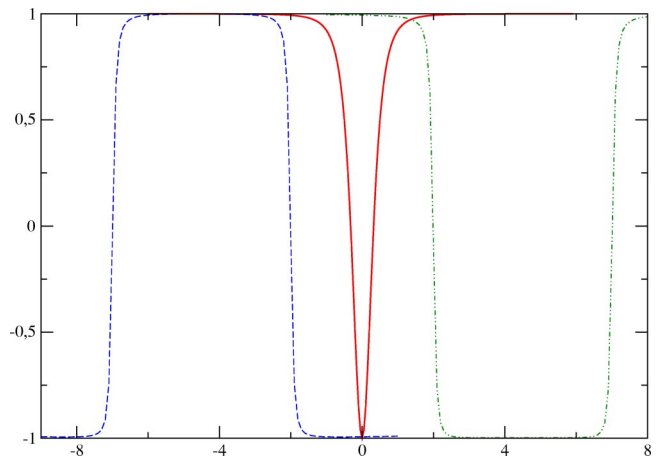
FIG. 1. Polyakov loop $P(x,0,0)$ as a function of x. The solid line corresponds to one instanton centered at the origin. The dashed and dotted-dashed lines show the results for a meron-meron pair located on the x axis at $x = -7,-2$ and an antimeron-meron pair at $x = 2,7$.

superposition of singular gauge instantons. In contrast, the tunneling process described by a single meron changes the sign of the Polyakov loop, as can be seen from the figure. Furthermore, the asymptotic values of P for a meron-antimeron pair and a meron-meron pair are of opposite sign. Thus, merons do not single out Polyakov loops of a definite sign and therefore have the potential of generating a center-symmetric ensemble.

II. MERON EFFECTIVE THEORY

In this work we explore the idea that merons are the essential degrees of freedom in SU(2) Yang-Mills gauge theory by writing the partition function as a path integral of an effective action, depending on the positions and color orientations of an ensemble of merons,

$$Z = \int \mathrm{d}z_i \mathrm{d}h_i e^{-(1/g^2)S[A(z_i, h_i)]}. \tag{1}$$

The gauge field for a meron in Lorentz gauge with its center at the origin, after the appropriate choice of the coordinate system in color space and after regularization of the singularity, is given by

$$a_\mu(x) = \frac{\eta_{a\mu\nu} x_\nu}{x^2 + \rho^2} \frac{\sigma^a}{2}. \tag{2}$$

Color and space-time dependence are correlated via the 't Hooft tensor $\eta_{a\mu\nu}$ [3]. For the vanishing meron size ρ, $a(x)$ is a solution of the Euclidean classical field equations [6]. Antimerons differ in sign if one of the space-time indices is 0. The action density of merons and antimerons is given by

$$s(x) = \frac{1}{2} \mathrm{tr} F_{\mu\nu} F_{\mu\nu} = \frac{3}{2(x^2 + \rho^2)^4}[x^4 + 4x^2\rho^2 + 8\rho^4]. \tag{3}$$

Unlike instantons, the field strength decays asymptotically as $1/x^2$, giving rise to an infrared logarithmic singularity in the action. For vanishing meron size, the action is also logarithmically divergent in the ultraviolet, so we will use ρ as an ultraviolet regulator. The topological charge density of a meron or antimeron

$$\tilde{s}(x) = \pm \frac{1}{2} \mathrm{tr} F_{\mu\nu} \tilde{F}_{\mu\nu} = \pm \frac{6\rho^2}{(x^2 + \rho^2)^4}[x^2 + 2\rho^2] \tag{4}$$

leads to a finite, size-independent topological charge

$$\nu = \frac{1}{8\pi^2} \int \mathrm{d}^4 x \tilde{s}(x) = \pm \frac{1}{2}. \tag{5}$$

The meron ensembles to be considered in this study contain field configurations obtained by superposition of merons and antimerons of fixed and equal number $N_M/2$,

$$A_\mu(x) = \sum_{i=1}^{N_M} h(i) a_\mu[x - z(i)] h^{-1}(i). \tag{6}$$

Such a configuration is specified by the position of the centers $z(i)$ and the color orientations

$$h(i) = h_0(i) + i\mathbf{h}(i) \cdot \boldsymbol{\sigma}, \quad h_0^2(i) + \mathbf{h}^2(i) = 1. \tag{7}$$

In the ensembles to be discussed, the location of the merons is restricted to a hypercube

$$-1 \leq z_\mu(i) \leq 1, \quad V = 16.$$

We identify the effective action in Eq. (1) with the Yang-Mills action. Our standard choice for meron size and coupling constant is

$$\rho = 0.16, \quad g^2 = 32.$$

It is essential to note that the infrared divergence of the action of a single meron does not prevent the construction of physical ensembles having an extensive action with a large number of merons. For instance, with the following choice of the color orientations of a system of four merons (or four antimerons)

$$h_k(i) = \delta_{i-1,k}, \tag{8}$$

the action density decays as $1/x^6$.

The meron ensembles have been generated by the Monte Carlo sampling of the action in the path integral, Eq. (1). In each step of a Metropolis update, the position and color orientation of a given meron are tentatively changed, the induced changes in the action density are evaluated at a set of mesh points distributed over the whole volume, and the configuration is accepted or rejected based on the global change in action. The long range nature of the meron fields makes the changes extend throughout the whole system.

We first present the results for the central quantity in the discussion of confinement, the Wilson loop

$$W = \frac{1}{2} \mathrm{tr} \left\{ P \exp i \oint_C \mathrm{d}x^\mu A_\mu(x) \right\}. \tag{9}$$

The integral is ordered along the closed path C. Our standard choice is a rectangular path located in an (x_i, x_j) plane with the center at the origin and with the ratio of the sides equal to 2. For a given configuration, we evaluate 12 different Wilson loops W_{ij} and obtain our final results by taking the ensemble average and the average over the 12 orientations. The statistical errors are calculated from the variance of the 12 orientations. Figure 2 shows the universal behavior of Wilson loops calculated with meron ensembles with a range of meron numbers. After rescaling the area $\mathcal{A} \rightarrow \lambda \mathcal{A}$, the values of the Wilson loop lie on a universal scaling curve, where deviations from scaling are within the statistical uncertainties. For loops that are not too small, the universal curve can be parametrized by the sum of a perimeter term and an area term

$$\ln\langle W \rangle = \omega + \tau \sqrt{\lambda} \mathcal{P} - \sigma \lambda \mathcal{A} \tag{10}$$

as shown in Fig. 2. The values of the parameters are
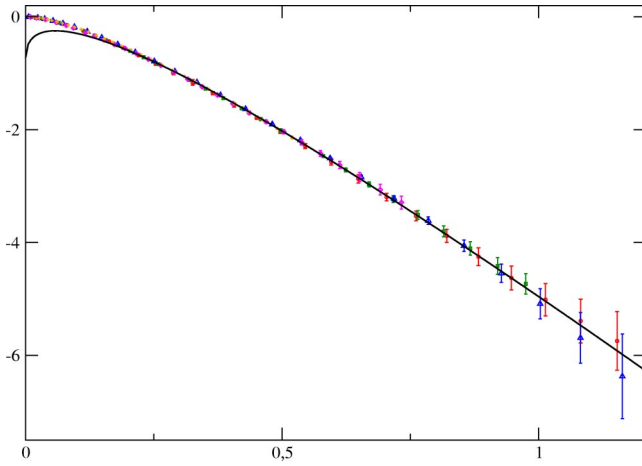
FIG. 2. Logarithm of Wilson loop as function of area $\mathcal{A}$. The data correspond to meron ensembles at $g^2 = 32$ with $N_M = 1000$, 500, 200, 100, and 50. The area has been rescaled by 1.86, 1.41, 1.0, 0.75, and 0.53, respectively. The line shows the fit with Eq. (10).

$$\omega = -0.72, \quad \tau = 0.93, \quad \sigma = 8.17. \tag{11}$$

The concave shape of $\ln\langle W \rangle$ as a function of the area arises from the difference in sign between the area and perimeter terms and makes the presence of a positive string tension unambiguous. Numerical results also confirm the expected increase of the Wilson loop with increasing perimeter at fixed area. These results thus demonstrate confinement in these meron ensembles.

III. TOPOLOGICAL SUSCEPTIBILITY AND ACTION DENSITY

In view of this impressive scaling behavior, it is useful to scale all subsequent results with a physical scale set by the string tension. For convenience in thinking about physical magnitudes, although we are considering SU(2), we will identify the value of σ with the physical value 4.2 fm^{-2} of the string tension. Ultimately we will compare dimensionless ratios involving powers of σ with SU(2) lattice results, so that this arbitrary physical scale in no way affects our quantitative results. Thus, our unit of length (u.l.) is converted to physical units by

$$1 \text{ u.l.} = 1.4\sqrt{\lambda} \text{ fm.} \tag{12}$$

Table I summarizes our principal results for the action density $\langle s \rangle$, and the topological susceptibility χ calculated in meron ensembles for different values of the meron density $n_M = N_M/V$ and scaled to the string tension. A striking feature is the fact that the action density and topological susceptibility depend essentially on a single scale, which we have chosen as the string tension. Indeed, despite the changes in the number of merons by up to a factor of 20, and of meron size and meron density by factors of 2 and 3, respectively, the action density and topological susceptibility vary by less than $\pm 5\%$. The results turn out to be similarly insensitive to

TABLE I. Meron density, meron size, action density and topological susceptibility for meron ensembles containing $N_M = 1000$, 500, 200, 100 and 50 merons.

n_M (fm^{-4})	ρ (fm^{-1})	$\langle s \rangle$ (fm^{-4})	$\chi^{1/4}$ (MeV)
4.8	0.30	222	123
4.1	0.26	234	121
3.3	0.22	237	126
2.9	0.19	238	126
2.9	0.16	240	128

large changes in the coupling constant. Hence, we will write the action density and topological susceptibility as

$$\langle s \rangle = 13.1\sigma^2 \tilde{s}(n\rho^4, g^2),$$

$$\chi^{1/4} = 0.31\sigma^{1/2}\tilde{\chi}^{1/4}(n\rho^4, g^2), \tag{13}$$

where, within 5% $\tilde{s} \approx 1$, $\tilde{\chi}^{1/4} \approx 1$. In the regime of parameters investigated, breaking the scale invariance of the meron fields by the introduction of the meron size ρ appears to have an effect similar to that of introducing a finite lattice size in the quantum theory. In both cases, the underlying scale invariance manifests itself in the appearance of logarithmic singularities for vanishing coordinate space regulators.

To understand the interplay between meron size and meron density we observe that the action density in the center of a meron [cf. Eq. (3)] is much larger than the average action density in the meron ensembles

$$\left.\frac{s(0)}{\langle s \rangle} = \frac{0.87}{\rho^4\sigma^2}\right|_{\rho = 0.25 fm} = 13.5. \tag{14}$$

This suggests a separation of the action density into background and meron peak contributions,

$$\langle s \rangle = s_B + s_M. \tag{15}$$

The meron peak contribution is obtained by integrating $s(x)$ [Eq. (3)] over a sphere of radius r, which for small meron size ($\rho \ll r$) becomes

$$s_M = n\int^r d^4x\, s(x) \to 3\pi^2 n\left(\frac{5}{12} + \ln\frac{r}{\rho}\right). \tag{16}$$

The matching requirement on r

$$s(r) = s_B \tag{17}$$

yields the following expression for the action density:

$$\langle s \rangle = \left[s_B + n\frac{3\pi^2}{4}\left(\frac{5}{3} - \ln\frac{2}{3}s_B\rho^4\right)\right].$$

This expression makes explicit the logarithmic singularity of $\langle s \rangle$ with the meron size in the small ρ limit if s_B is identified with the physical (i.e. regularized) value of the action den-

sity. With the action density s as an input (cf. Table I), the relative strength of the background contribution can be determined numerically

$$\frac{s_B}{\langle s \rangle} = 0.65 - 0.75.$$

This result indicates that a significant fraction of the action density is associated with the logarithmically singular contribution in Eq. (16).

We can now compare the meron results in Eq. (13) with known QCD results. The topological susceptibility

$$\chi = \left(\frac{1}{32\pi^2} \right)^2 \int \mathrm{d}^4 x \langle F_{\mu\nu}^a \widetilde{F}_{\mu\nu}^a(x) F_{\mu\nu}^a \widetilde{F}_{\mu\nu}^a(0) \rangle \qquad (18)$$

is a robust quantity that can be measured unambiguously in our effective theory and in lattice QCD. It has a direct physical interpretation because of its relation to the η' mass by the Veneziano-Witten formula. The most extensive lattice measurement of the $SU(2)$ topological susceptibility by extracting the continuum limit from calculations over a large range of the coupling constant [7] yields $\chi^{1/4}/\sigma^{1/2} \sim 0.483 \pm .006$. The meron result $\chi^{1/4}/\sigma^{1/2} \sim 0.31$ from Eq. (13) is in qualitative agreement with this lattice result. Note that χ can be computed reliably for the meron ensembles since the topological charge of a single meron, Eq. (5), is finite. The topological susceptibility is dominated by the short-range peaks in the topological charge density associated with individual merons and antimerons, and not by the long range background field. The contribution due to single peaks yields

$$\chi^{1/4} = 0.505 n_M^{1/4}. \qquad (19)$$

The weak variation in $\chi^{1/4}$ and the magnitude of this estimate are in qualitative agreement with the results of Table I.

Because of the necessity of subtracting divergent terms to define the continuum limit, the action density, or equivalently the gluon condensate, is more difficult than the topological susceptibility to evaluate accurately in either QCD or a meron ensemble. Lattice $SU(2)$ calculations for the action density range from $\langle s \rangle / \sigma^2 = 4.5$ [8] to 25.3 [9] and QCD sum rule results range from $\langle s \rangle / \sigma^2 = 4.5$ [10] to 10 [11]. The meron result $\langle s \rangle / \sigma^2 \sim 13.1$ from Eq. (13) is thus consistent with our present knowledge of the action density. It is useful

to note that in the lattice calculations of Ref. [8], the divergent contributions are about a factor of 20–500 larger than the extracted value of $\langle s \rangle$. As noted above, the meron action density also contains a divergent contribution that, if subtracted, will significantly reduce the value of the condensate given in Table I.

IV. CONCLUSIONS

In conclusion, we have shown that an effective theory with meron degrees of freedom succeeds in describing essential features of QCD. The long-range gauge fields provide the correlations and disorder needed for confinement while the short range fluctuations play an essential role in other physical observables. They render the meron dynamics more complicated than for ensembles of weakly interacting singular gauge instantons and must therefore be treated numerically. The central feature and a major success of this approach is producing confinement. We have demonstrated a confining area law and discussed how a meron ensemble may implement center symmetry. We also observe scaling behavior, reminiscent of lattice Yang-Mills theory which might not *a priori* have been expected. In our effective theory there are three parameters, g^2, ρ, and n_M, and one combination of ρ and n_M is determined by fitting to the string tension at a given g^2. The action density and topological charge density are rather insensitive to the other combination and the Wilson loops scale to a universal curve. This scaling behavior is presumably connected with the scale invariance of the multi-meron action in the limit $\rho \to 0$. In addition, we have shown qualitative agreement with the topological susceptibility and action density measured in SU(2) lattice QCD.

[1] L.G. Yaffe and B. Svetitsky, Phys. Rev. D **26**, 963 (1982).

[2] B. Svetitsky, Phys. Rep. **132**, 1 (1986).

[3] T. Schäfer and E.V. Shuryak, Rev. Mod. Phys. **70**, 323 (1998).

[4] J.W. Negele, Nucl. Phys. B (Proc. Suppl.) **73**, 92 (1999).

[5] C.G. Callan, R.F. Dashen, and D.J. Gross, Phys. Rev. D **19**, 1826 (1979); **17**, 2717 (1978); Phys. Lett. **66B**, 375 (1977).

[6] V. de Alfaro, S. Fubini, and G. Furlan, Phys. Lett. **65B**, 163 (1976).

[7] B. Lucini and M. Teper, J. High Energy Phys. **06**, 050 (2001).

[8] M. Campostrini, A. Di Giacomo, and G. Paffuti, Z. Phys. C **22**, 143 (1984).

[9] A. Di Giacomo, H. Panagopoulos, and E. Vicari, Nucl. Phys. **B338**, 294 (1990).

[10] M.A. Shifman, A.I. Vainshtein, and V.I. Zakharov, Nucl. Phys. **B147**, 385 (1979).

[11] S. Narison, Phys. Lett. B **387**, 162 (1996).